Novel Coordination Behavior of *fac*-$[ReBr_3(CO)_3]^{2-}$ with 1,3,5-Triaza-7-phosphaadamantane (PTA). Systematic Investigation on Stepwise Replacement of the Halides by PTA Ligand. Phase Transfer Studies and X-ray Crystal Structure of $[NEt_4][ReBr_2((PTA)(CO)_3]$, $[ReBr(PTA)_2(CO)_3]$, and $[Re(PTA)_3(CO)_3]PF_6$

Roger Schibli,[†] Kattesh V. Katti,*[,†] Wynn A. Volkert,[‡] and Charles L. Barnes[§]

Department of Radiology and Center for Radiological Research, Business Loop 70 West, Allton Bldg. Room 106, Columbia, Missouri 65211, H. S. Truman Memorial V. A. Hospital, Columbia, Missouri 65203, and Department of Chemistry, University of Missouri—Columbia, Columbia, Missouri 65211

Received April 3, 1998

Starting originally from $[NEt_4]_2[ReBr_3(CO)_3]$ (**1**), the three novel complexes $[NEt_4][ReBr_2(PTA)(CO)_3]$ (**2**), $[ReBr(PTA)_2(CO)_3]$ (**3a**), and $[Re(PTA)_3(CO)_3]PF_6$ (**4**) (PTA = 1,3,5-triaza-7-phosphaadamantane) were prepared and characterized by IR, ^1H, ^{13}C, and ^{31}P NMR spectroscopy and X-ray crystallography. These complexes are the first representatives of mixed carbonyl/PTA complexes of an element of the manganese row. All substitution reactions have been performed under aerobic conditions at ambient temperature and the yields were in all the cases high. The disubstituted complex was isolated as the neutral species **3a** and as the dicationic species $[ReBr(PTAH)_2(CO)_3]Br_2$, **3b**, which is protonated at one amine group of each of the two PTA ligands. The substitution reaction leading to the formation of **3a** was performed in H_2O, methanol and DMSO/methanol (4:1) and the reaction was followed using ^{31}P NMR techniques. These experiments revealed that the number and concentration of intermediate species during the substitution reaction are strongly dependent on the solvent system. Furthermore due to a completely different solubility behavior of **3a** and **3b**, a fully reversible phase transfer of the disubstituted complex from the organic (THF) to the aqueous layer (2 M NaBr) and back could be induced by simply changing the pH of the aqueous phase. In the ^{31}P NMR experiment, the existence of the monoprotonated species $[ReBr(PTA)(PTAH)(CO)_3]Br$ (**3c**) could also be detected. X-ray data for complex **2**: monoclinic $P2_1/n$, $a = 8.6889(4)$ Å, $b = 29.3089(14)$ Å, $c = 9.3017(5)$ Å, $\beta = 97.1520(10)°$, $Z = 4$, $R/R_w = 0.048/0.079$. X-ray data for complex **3a**: monoclinic $P2_1/c$, $a = 6.8581(40$ Å, $b = 21.9499(12)$ Å, $c = 13.9526(8)$ Å, $\beta = 94.6650(10)°$, $Z = 4$, $R/R_w = 0.036/0.042$. X-ray data for complex **3b**: triclinic $P\bar{1}$, $a = 8.7051(5)$ Å, $b = 11.9307(7)$ Å, $c = 14.7458(8)$ Å, $\alpha = 78.9450(10)°$, $\beta = 87.2340(10)°$, $\gamma = 76.4770(10)°$, $Z = 2$, $R/R_w = 0.034/0.042$. X-ray data for complex **4**: triclinic $P\bar{1}$, $a = 9.3842(50)$ Å, $b = 13.5797(7)$ Å, $c = 13.9499(7)$ Å, $\alpha = 105.5910(10)°$, $\beta = 91.8560(10)°$, $\gamma = 107.0190(10)°$, $Z = 2$, $R/R_w = 0.051/0.062$.

Introduction

The preparation of water-soluble, organometallic transition metal complexes has recently received considerable attention for applications in different areas. Predominantly, the research efforts focus on the development of water-soluble compounds for liquid/liquid biphasic catalysis and heterogeneous catalysis as documented in several review articles.[1] The application of catalytically active metal centers in aqueous media enables not only an easy separation and recovery of the expensive catalyst from the substrate and products but is also important from an ecological/economical point of view since water is an environmentally benign and inexpensive solvent. Nuclear medicine and radiopharmacy are other fields where water solubility of metal complexes is favorable because of their better in vivo characteristics (e.g., faster clearance of the drug through the urinary pathway). Remarkable progress was made in the past few years on the synthesis of water-soluble complexes with diagnostic (e.g. Tc-99m)[2] and therapeutic (e.g. Au-198/199) radionuclides.[3] In both fields of research (catalysis and radiopharmacy), the water solubility is usually attained utilizing a variety of water-soluble ligand systems and, in particular, ternary organophosphorus ligands such as sulfonated phosphines,[4] 1,3,5-triaza-7-phosphaadamantane (PTA),[5a−d] tris(hydroxymethyl)phosphine (THP)[3] or bis(bis(hydroxymethyl)phosphino)ethane (HMPE).[6] In an effort to develop new organometallic precursors for radiopharmaceutical applications, Alberto and co-workers recently published a new normal pressure synthesis for the organometallic precursors $[NEt_4]_2[MX_3(CO)_3]$ (M = Tc, Re; X = Cl,

* Author for correspondence. Fax: (573) 884-5679. E-mail: radkatti@showme.missouri.edu.
[†] Department of Radiology and Center for Radiological Research.
[‡] H. S. Truman Memorial V. A. Hospital.
[§] Department of Chemistry.

(1) Joo, F.; Toth, Z. *J. Mol. Catal.* **1980**, *8*, 369. Herrmann, W. A.; Cornils, B. *Angew. Chem., Int. Ed. Engl.* **1997**, *36*, 1048. Herrmann, W. A.; Kohlpainter, C. W. *Angew. Chem., Int. Ed. Engl.* **1993**, *32*, 1524.
(2) Berning, D. E.; Katti, K. V.; Singh, P. R.; Higgenbotham, C.; Reddy, V. S.; Volkert, W. A. *Nucl. Med. Biol.* **1996**, *23*, 617. Scott Edwards, D.; Liu, S.; Barrett, J. A.; Harris, A. R.; Looby, R. J.; Ziegler, M. C.; Heminway, S. J.; Carroll, T. R. *Bioconjugate Chem.* **1997**, *8*, 146.
(3) Berning, D. E.; Katti, K. V.; Barnes, C. L.; Volkert, W. A. *Chem. Ber.* **1997**, *130*, 907.
(4) Darensbourg, D. J.; Bischoff, C. J. *Inorg. Chem.* **1993**, *32*, 47. Kuntz, E. G. *Chemtech* **1987**, *17*, 570.

S0020-1669(98)00373-5 CCC: $15.00
Published on Web 09/05/1998

Br).[7a,b] $[NEt_4]_2[ReBr_3(CO)_3]$ (**1**) as well as the corresponding technetium complex analogue have proved to be highly stable and water soluble.[8]

As part of our ongoing studies on the development of fundamental chemistry of water-soluble organometallic Tc(I) and Re(I) compounds for potential use in radiopharmaceutical applications, we are currently investigating the coordination chemistry of organorhenium/technetium complexes with water-soluble phosphine ligands. The low steric requirements coupled with the high-oxidative stability and water solubility of 1,3,5-triaza-7-phosphaadamantane prompted a systematic investigation of ligand substitution on $[NEt_4]_2[ReBr_3(CO)_3]$. We, herein, report the synthesis, spectroscopic and solution behavior and the X-ray crystallographic investigation of the complexes $[NEt_4][ReBr_2(PTA)(CO)_3]$ (**2**), $[ReBr(PTA)_2(CO)_3]$ (**3a**) $[ReBr(PTAH)_2(CO)_3]Br_2$ (**3b**), and $[Re(PTA)_3(CO)_3]PF_6$ (**4**).

Experimental Section

All manipulations were carried out under aerobic conditions. Solvents were purchased from Fisher Scientific and dried by standard methods. 1,3,5-Triaza-7-phosphaadamantane (PTA) was synthesized as described by Daigle and co-workers.[9] The metal precursor $[NEt_4]_2[ReBr_3(CO)_3]$ (**1**) was synthesized according to the previously reported literature method.[7a] NMR spectra were recorded on a Bruker ARX-300 spectrometer. The ^1H and ^{13}C chemical shifts are reported relative to residual solvent protons as a reference, while the ^{31}P shifts are reported relative to an external reference of 85% H_3PO_4. IR spectra were recorded on a Galaxy Series FTIR 3000 using KBr pellets. Elementary Analyses were performed by Oneida Research Service, Inc. (Whitesboro, NY).

Synthesis of $[NEt_4][ReBr_2(PTA)(CO)_3]$ (2). To a methanolic solution (10 cm^3) of **1** (96 mg, 0.12 mmol) was added PTA (20 mg, 0.12 mmol), and the solution stirred for 3 h. The solvent was removed in vacuo, the residue was extracted with 10 cm^3 of dry THF, and the solution was filtered. Layering the filtrate with diethyl ether yielded colorless crystals of the product. Yield: 74 mg (82%). Elementary anal. Calcd for $C_{17}H_{32}N_4O_3Br_2PRe$: C, 28.46; H, 4.49; N, 7.81. Found: 27.97; 4.10; 7.69. IR (cm^{-1}, KBr): 2987 (w), 2958 (w), 2009 (vs), 1892 (vs), 1462 (m), 1253 (m), 1026 (m), 999 (m), 804 (w), 769 (w). ^1H (δ, acetonitrile-d_3): 4.53 (d, 3 H, NCH_{ax}N, J_{HH} = 12.9 Hz), 4.45 (d, 3 H, NCH_{eq}N, J_{HH} = 12.9 Hz), 4.24 (s, 6 H, PCH_2N), 3.20 (q, 8 H, CH_2, J_{HH} = 7.23 Hz), 1.23 (tt, 12 H, CH_3, J_{HH} = 7.23 Hz, J_{NH} = 1.74 Hz). ^{13}C (δ, acetonitrile-d_3): 73.0 (s, NCH_2N), 52.5 (s, CH_2), 50.7 (d, PCH_2N, J_{PC} = 17.4 Hz), 7.2 (s, CH_3). ^{31}P (δ, acetonitrile-d_3): −87.7 (s).

Synthesis of $[ReBr(PTA)_2(CO)_3]$ (3a). PTA (49 mg, 0.29 mmol) was added to an aqueous solution (5 cm^3) of **1** (105 mg, 0.13 mmol), and the reaction was stirred for 12 h, during which time a white precipitate of the product was formed. The solution was filtered and the residue dried in vacuo. Yield: 79 mg (91% based on Re). Elementary anal. Calcd for $C_{15}H_{24}N_6O_3P_2BrRe$: C, 27.11; H, 3.64; N, 12.64. Found: 26.69, 4.21, 12.22. IR (cm^{-1}, KBr): 2936 (w), 2029 (vs), 1941 (vs), 1902 (vs), 1292 (w), 1244 (w), 1105 (w), 1022 (m), 978 (m), 951 (m), 810 (w), 586 (w); ^1H (δ, acetone-d_6): 4.64 (s, 12 H, PCH_2N), 4.39 (d, 6 H, NCH_{ax}N, J_{HH} = 14.8 Hz), 4.31 (d, 6 H, NCH_{eq}N, J_{HH} = 14.8 Hz); ^{13}C (δ, acetone-d_6): 71.0 (s, NCH_2N), 52.1 (virtual triplet, PCH_2N, J_{PC} = 9.8 Hz); ^{31}P (δ, acetone-d_6): −91.9 (s).

Synthesis of $[ReBr(PTAH)_2(CO)_3]Br_2$ (3b). Complex **3b** was synthesized by two different protocols.

Procedure A. To a methanolic suspension of **3a** was added 2 equiv of concentrated HBr (48%). Subsequent removal of the solvent yielded the product almost quantitatively.

Procedure B. To a suspension of **1** (92 mg, 0.12 mmol) in 10 cm^3 dry THF 10 was added 2 equiv of $AgPF_6$ (58 mg, 0.23 mmol) dissolved in 2 cm^3 THF. The solution was stirred for 2 h. After filtration, 2 equiv of PTA (40 mg, 0.24 mmol) was added to the filtrate and the solution stirred for an other 3 h at ambient temperature. Addition of 3 equiv concentrated HBr (40 μL, 0.36 mmol) yielded the analytical pure product as a thick white precipitate that was filtered and dried in vacuo. Yield: 93 mg (93% based on Re). Elementary anal. Calcd for $C_{15}H_{26}N_6O_3Br_3P_2Re$: C, 21.80; H, 3.17: N, 10.17. Found: 21.57; 2.96; 10.39. IR (cm^{-1}, KBr): 3443 (w), 2953 (w), 2878 (w), 2768 (w), 2608 (w), 2564 (w), 2041 (vs), 1966 (vs), 1921 (vs), 1452 (w), 1308 (m), 1119 (w), 1026 (m), 982 (m), 949 (m), 899 (w), 814 (w), 772 (w). ^1H (δ, D_2O): 4.80 (s, 12 H, PCH_2N), 4.41 (d, 6 H, NCH_{ax}N, J_{HH} = 15.2 Hz), 4.34 (d, 6 H, NCH_{eq}N, J_{HH} = 15.2 Hz). ^{13}C (δ, D_2O): 71.1 (s, NCH_2N), 50.0 (virtual triplet, PCH_2, J_{PC} = 9.1 Hz). ^{31}P (δ, D_2O): −75.2 (s).

Synthesis of $[Re(PTA)_3(CO)_3]PF_6$ (4). To a suspension of **1** (126 mg, 0.16 mmol) in 10 cm^3 of dry THF was added 3 equiv of $AgPF_6$ (123 mg, 0.49 mmol) diluted in 2 cm^3 of dry THF. The solution was stirred for 2 h. After filtration of AgBr, 3 equiv of PTA (82 mg, 0.49 mmol) was added to the filtrate, and the solution was stirred for 15 h at ambient temperature. Following solvent removal in vacuo, the residue was recrystallized from acetonitrile/diethyl ether. Yield: 110 mg (75% based on Re). Calcd for $C_{21}H_{36}N_9O_3F_6P_4Re$: C, 28.44; H, 4.09; N, 14.21. Found: 28.58; 3.98; 14.37. IR (cm^{-1}, KBr): 3443 (w), 2950 (w), 2056 (vs), 1968 (vs), 1451 (w), 1296 (m), 1244 (w), 1103 (w), 1018 (m), 974 (s), 949 (m), 847 (s), 581 (w). ^1H (δ, acetonitrile-d_3): 4.68 (d, 9 H, NCH_{ax}N, J_{HH} = 13.5 Hz), 4.61 (d, 9 H, NCH_{eq}N, J_{HH} = 13.5 Hz), 4.29 (s, 18 H, PCH_2N). ^{13}C (δ, acetonitrile-d_3): 72.0 (s, NCH_2N), 55.1 (broad s, PCH_2). ^{31}P (δ, acetonitrile-d_3): −95.2 (broad s, PTA); −144.1 (septet, PF_6^-).

X-ray Data Collection and Processing. Details of the data collection, structure solution, and refinement for complexes **2**, **3a**/**b**, and **4** are summarized in Table 1. The intensity data were collected on a Siemens SMART CCD system using the ω scan mode. Data were corrected for decay and absorption using the program SADABS based on the method of Blessing.[10] The structures were solved using the program SHELX S86[11] and refined on the NRCVAX system.[12] All hydrogen atoms were placed at the idealized positions. Atomic coordinates and their equivalent isotropic displacement coefficients for all compounds are included in the Supporting Information. Cubic, colorless crystals of X-ray-quality of compound **2** were obtained by slow diffusion of hexane into a THF solution of the compound. Crystals of **3a** grow as long, colorless needles from a hot methanolic solution upon slow cooling to ambient temperature, whereas crystals of **3b** were obtained from a hot saturated THF solution. Compound **4** crystallized from an acetonitrile solution layered with diethyl ether.

(5) (a) Darensbourg, D. J.; White Stafford, N.; Joó, F.; Reibenspies, J. H. *J. Organomet. Chem.* **1995**, *488*, 99. (b) Darensbourg, D. J.; Joo, F.; Kannisto, M.; Katho, A.; Reibenspies, J. H. *Organometallics* **1992**, *11*, 1990. (c) Darensbourg, D. J.; Decuir, T. J.; White Stafford, N.; Robertson, J. B.; Draper, J. D.; Reibenspies, J. H.; Katho, A.; Joo, F. *Inorg. Chem.* **1997**, *36*, 4218. (d) Darensbourg, D. J.; Joó, F.; Kannisto, M.; Kathó, A.; Reibenspies, J. H.; Daigle, D. J. *Inorg. Chem.* **1994**, *33*, 200.

(6) Reddy, V. S.; Katti, K. V.; Barnes, C. L. *Inorg. Chim. Acta* **1995**, *240*, 367. Berning, D. E.; Katti, K. V.; Barnes, C. L.; Volkert, W. A.; Ketring, A. R. *Inorg. Chem.* **1997**, *36*, 2765.

(7) (a) Alberto, R.; Schibli, R.; Egli, A.; Schubiger, P. A.; Herrmann, W. A.; Artus, G.; Abram, U.; Kaden, T. A. *J. Organomet. Chem.* **1995**, *493*, 119. (b) Alberto, R.; Schibli, R.; Schubiger, P. A.; Abram, U.; Kaden, T. A. *Polyhedron* **1996**, *15*, 1079.

(8) Egli, A.; Hegetschweiler, C.; Alberto, R.; Abram, U.; Schibli, R.; Hedinger, R.; Gramlich, V.; Kissner, R.; Schubiger, P. A. *Organometallics* **1997**, *16*, 1833.

(9) Daigle, D. J.; Pepperman, A. B.; Vail, S. L. *Heterocyl. Chem.* **1974**, *11*, 407.

(10) Blessing, R. H. *Acta Crystallogr.* **1995**, *A51*, 33.

(11) Sheldrick, G. M. *SHELXS86*: *A program for the resolution of X-ray structures*; Universitiy of Göttingen: Göttingen, Germany, 1986.

(12) Gabe, E. J.; Le Page, Y.; Charland, J.-P.; Lee, F. L.; White, P. S. *J. Appl. Crystallogr.* **1989**, *22*, 384. Johnson, C. K.: *ORTEP*: *A Fortran thermal ellipsoid plot program*; Technical Report ORNL-5138; Oak Ridge National Laboratory: Oak Ridge, TN, 1976. Le Page, Y. *J. Appl. Crystallogr.* **1988**, *21*, 983. Le Page, Y.; Gabe, E. J. *J. Appl. Crystallogr.* **1979**, *12*, 464.

Table 1. Crystal Data and Details of Data Collection for Complexes **2**, **3a**, **3b**, and **4**

compound	**2**	**3a**	**3b**	**4**
empirical formula	$C_{17}H_{32}N_4O_3PBr_2Re$	$C_{15}H_{24}N_6O_3P_2BrRe$	$C_{19}H_{32}N_6O_4P_2Br_3Re$	$C_{23}H_{39}N_{10}O_3F_6P_4Re$
space group	$P2_1/n$	$P2_1/c$	$P1$	$P1$
fw	717.46	700.48	896.36	927.72
a [Å]	8.6889(4)	6.8581(4)	8.7051(5)	9.3842(5)
b [Å]	29.3089(14)	21.9499(12)	11.9307(7)	13.5797(7)
c [Å]	9.3017(5)	13.9526(8)	14.7458(8)	13.9499(7)
α [deg]	90	90	78.9450(10)	105.5910(10)
β [deg]	97.1520(10)	94.6650(10)	87.2340(10)	91.8560(10)
γ [deg]	90	90	76.4770(10)	107.0190(10)
μ [cm^{-1}]	0.870	0.795	0.842	0.406
V [Å^3]	2350.36(20)	2093.39(21)	1461.37(14)	1625.36(15)
ρ_{calcd} [g/cm^3]	2.028	2.108	2.037	1.896
λ [Å]	0.710 73	0.710 73	0.710 73	0.710 73
Z	4	4	2	2
temp [K]	173	173	173	173
R_w/R_1[a]	0.079/0.048	0.042/0.036	0.042/0.034	0.062/0.051

[a] $R_w = [\sum w(|F_o| - |F_c|)^2|)/\sum(w(|F_o|^2)|)]^{1/2}$; $R = \sum(||F_o| - |F_c||)/\sum(|F_o|)$.

Scheme 1

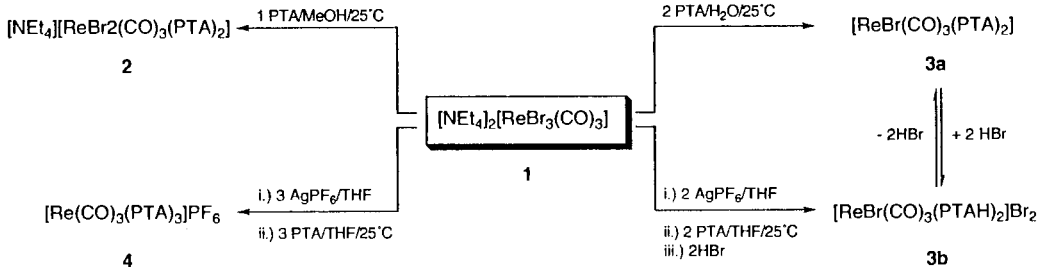

Results and Discussion

It is important to recognize that, to date, there were no reports on carbonyl complexes of the elements of the manganese row with the PTA ligand. This lack of studies is striking since the corresponding compounds of most of the neighboring transition metals of groups 6 and 8 have been known for a long time and are still the topic of current investigations.[13,14a,b] The compounds reported in this paper are the first organometallic representatives of a group 7 element for this class of ligands and, therefore, close an important gap.

Synthesis and Characterization of $[NEt_4][ReBr_2(PTA)(CO)_3]$ (2). Utility of the synthon $[NEt_4]_2[ReBr_3(CO)_3]$ (**1**), rather than the rhenium(I) halopentacarbonyl, has decisive advantages: (1) complex **1** is not only soluble in organic solvents but also in water; (2) the desired *fac*-$Re(CO)_3$ moiety is already preformed, thus no CO has to be displaced employing harsh reaction conditions; (3) the three halides in **1** are easy to substitute by other ligand systems. Stirring a methanolic solution of **1** with 1 equiv of PTA at room temperature produced $[NEt_4][ReBr_2(PTA)(CO)_3]$ within 3 h as confirmed by ^{31}P NMR experiments. The reaction pathway is outlined in Scheme 1. Compound **2** is soluble in most polar organic solvents but only slightly soluble in water. The ^{31}P NMR spectrum, recorded in acetonitrile, exhibits a singlet at −87.7 ppm which is significantly downfield shifted as compared to free PTA ligand ($\Delta\delta$ = 12.7 ppm). The ^{1}H NMR spectrum revealed two doublets with an AB pattern caused by the three $NCH_{ax}N$ and three $NCH_{eq}N$ protons and a singlet for the six PCH_2N protons. In addition the signals of the protons of counterion $[NEt_4]^+$ were observed in the right ratio. The IR spectrum (in KBr) revealed the typical "*fac*-$M(CO)_3$" pattern with C−O stretching absorptions at 2009 and 1892 cm^{-1}.

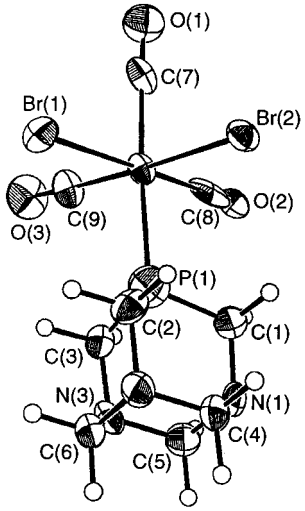

Figure 1. ORTEP drawing of the anion of $[NEt_4][ReBr_2(PTA)(CO)_3]$ (**2**) with atom numbering scheme. Ellipsoids are drawn on the 50% probability level.

The molecular structure of compound **2** was further confirmed by X-ray crystallography. An ORTEP view of the complex anion is shown in Figure 1 along with the atom-numbering scheme. Selected bond lengths and angles are listed in Table 2. $[NEt_4][ReBr_2(PTA)(CO)_3]$ crystallized in the monoclinic space group $P2_1/n$ with one formula unit in the asymmetric unit. The average Re−Br bond distance is 2.64(1) Å. The Re−C bond distances range from 1.896(9) Å (C9−Re) to 2.062(15) Å (C8−Re). The octahedral arrangement of the ligands deviates only slightly from the ideal values. The Br−Re−Br angle is

(13) Darensbourg, M. Y.; Daigle, D. *Inorg. Chem.* **1975**, *14*, 1217. DeLerno, J. R.; Trefonas, L. M.; Darensbourg, M. Y.; Majeste, R. J. *Inorg. Chem.* **1976**, *15*, 816.
(14) (a) Alyea, E. C.; Ferguson, G.; Kannan, S. *Polyhedron* **1997**, *16*, 3533. (b) Darensbourg, D. J.; Beckford, F. A.; Reibenspies, H. J. *Inorg. Chem.* **1997**, submitted for publication.

Table 2. Selected Bond Lengths (Å) and Angles (deg) of Compound **2**

Re−Br(1)	2.6297(10)	Re−C7	1.931(10)
Re−Br(2)	2.6530(8)	Re−C(8)	2.062(15)
Re−P(1)	2.321(4)	Re−C(9)	1.896(9)
Br(1)−Re−Br(2)	87.52(3)	Br(2)−Re−C(9)	174.9(3)
Br(1)−Re−P(1)	91.55(9)	P(1)−Re−C(7)	176.4(3)
Br(1)−Re−C(8)	177.6(3)	P(1)−Re−C(8)	89.5(3)
Br(1)−Re−C(7)	90.6(3)	P(1)−Re−C(9)	93.7(3)
Br(1)−Re−C(9)	87.3(3)	C(7)−Re−C(8)	88.5(4)
Br(2)−Re−P(1)	86.58(9)	C(7)−Re−C(9)	89.3(4)
Br(2)−Re−C(7)	90.59(25)	C(8)−Re−C(9)	90.5(4)
Br(2)−Re−C(8)	94.69(25)		

87.52(3)°, and the Br−Re−P and C−Re−C bond angles have averages of 89(3) and 89(1)° respectively.

Synthesis and Characterization of $[ReBr(PTA)_2(CO)_3]$ (3a) and $[ReBr(PTAH)_2(CO)_3]Br_2$ (3b). The synthetic strategy for the preparation of **3a** and **3b** (Scheme 1) profits from the completely different solubility behavior of the two products which will be discussed later. The neutral complex $[ReBr(PTA)_2(CO)_3]$ is formed in near quantitative yields in water or in polar organic solvents, from which it precipitates in analytical pure form as white fluffy needles. The spectroscopic data are in agreement with the proposed structure. The ^{31}P NMR spectrum in acetone exhibits a singlet at −91.9 ppm, and the ^1H NMR spectrum shows only the signals of the PTA ligands (singlet at 4.63 ppm and two doublets centered at 4.39 and 4.31 ppm). The C−O absorption bands are detected at 2029, 1941, and 1902 cm^{-1}.

The diprotonated complex $[ReBr(PTAH)_2(CO)_3]Br_2$ (**3b**) can be prepared by adding 2 equiv of HBr to a suspension of **3a** in water or methanol. Removal of the solvent and drying in vacuo yielded the product nearly in quantitative and analytically pure form. Complex **3b** can also be directly synthesized staring from **1**. Precipitation of two bromides of **1** with 2 equiv of $AgPF_6$ in THF produced $[ReBr(THF)_2(CO)_3]$. After filtration of AgBr, 2 equiv of PTA was added to the filtrate. Complex **3a** was formed within a few minutes, as confirmed by ^{31}P NMR experiments. After the addition of HBr to the clear reaction solution, **3b** precipitated quantitatively as a white fluffy powder. The C−O absorptions for **3b** were found at 2041, 1966, and 1921 cm^{-1} and are significantly blue-shifted compared to **3a**, presumably due to the double positive charge of the complex cation. This causes a weakening of the metal-to-carbonyl π-back-bonding. However, the C−O stretch bands in **3b** are less blue-shifted than in the monocationic complex **4** (2056 and 1968 cm^{-1}). Obviously the +2 overall charge of the complex cation is not completely delocalized over the whole molecule but is manly localized on the protonated ligands. This assumption is underlined by the fact that **3b** reveals a unexpected strong low field shift of the ^{31}P resonance (−75.3 ppm) compared to complexes **2**, **3a**, and **4**.

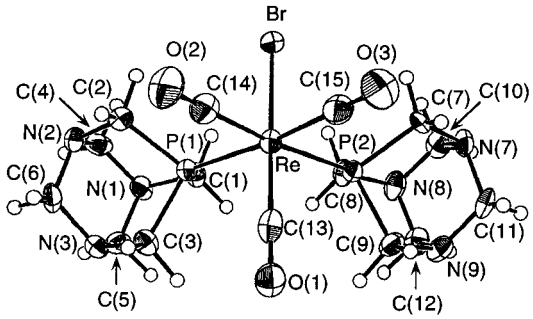

Figure 2. ORTEP drawing of $[ReBr(PTA)_2(CO)_3]$ (**3a**) with atom numbering scheme. Ellipsoids are drawn on the 50% probability level.

The neutral complex **3a** crystallized in the monoclinic space group $P2_1/c$. Selected bond lengths and angles are given in Table 3. The P−Re−P bond angle is with 98.62(5)° significantly enlarged. This deviation from the expected 90° for an octahedron is noteworthy since PTA has a small cone angle and steric hindrance should therefore be minimized. As a consequence, the P−Re−Br angles are narrowed (average of 84.0(7)°). Surprisingly the C−Re−C angles are not affected by this distortion and have an average of 91(2)°. The mean Re−P and Re−C bond distances are 2.44(1) and 1.94(3) Å, respectively. An ORTEP of **3a** is presented in Figure 2.

3b crystallized in the triclinic space group $P\bar{1}$. No significant structural differences between **3a** and **3b** around the rhenium center could be observed and thus, no separate ORTEP of **3b** is given. However, due to the protonation of one amine group at each PTA ligand, we could find two different sets of N−C bonds lengths. The quaternary nitrogens possess N−C distances with an average of 1.52(2) Å whereas the tertiary nitrogens N−C bonds are centered at 1.45(3) Å. It may be noted that similar observations were reported for the Ru, Rh, Ni, Pd, and Pt complexes with protonated PTA ligands.[5a,c,d] Both uncoordinated bromine atoms are involved in hydrogen bonding to one

Table 3. Selected Bond Lengths (Å) and Angles (deg) of Compound **3a**/**3b**

	3a	**3b**		**3a**	**3b**
Re−Br	2.6549(8)	2.6366(6)	N(2)−C(6)	1.462(10)	1.421(9)
Re−P(1)	2.447(2)	2.4287(15)	N(3)−C(3)	1.469(8)	1.504(8)
Re−P(2)	2.427(2)	2.4254(13)	N(3)−C(5)	1.463(10)	1.542(9)
Re−C(13)	1.914(8)	1.920(6)	N(3)−C(6)	1.487(9)	1.518(9)
Re−C(14)	1.966(7)	1.963(6)	N(7)−C(7)	1.491(9)	1.479(8)
Re−C(15)	1.950(7)	1.958(6)	N(7)−C(10)	1.472(10)	1.467(8)
P(1)−C(1)	1.858(7)	1.845(6)	N(7)−C(11)	1.481(9)	1.420(9)
P(1)−C(2)	1.851(7)	1.845(6)	N(8)−C(8)	1.460(8)	1.495(8)
P(1)−C(3)	1.851(7)	1.855(6)	N(8)−C(10)	1.467(10)	1.453(9)
P(2)−C(7)	1.852(6)	1.842(6)	N(8)−C(12)	1.460(10)	1.411(10)
P(2)−C(8)	1.833(7)	1.837(6)	N(9)−C(9)	1.473(9)	1.499(8)
P(2)−C(9)	1.833(6)	1.837(6)	N(9)−C(11)	1.464(9)	1.505(9)
N(1)−C(1)	1.487(8)	1.471(7)	N(9)−C(12)	1.454(10)	1.530(10)
N(1)−C(4)	1.474(10)	1.463(8)	O(1)−C(13)	1.148(10)	1.135(7)
N(1)−C(5)	1.459(9)	1.430(8)	O(2)−C(14)	1.128(9)	1.152(7)
N(2)−C(2)	1.487(9)	1.471(8)	O(30−C(15)	1.140(9)	1.144(7)
N(2)−C(4)	1.469(11)	1.463(8)			
Br−Re−P(1)	84.52(4)	88.19(4)	Br−Re−C(14)	94.05(23)	90.25(17)
Br−Re−P(2)	83.65(4)	84.92(4)	Br−Re−C(15)	92.49(24)	88.91(16)
Br−Re−C(13)	171.41(21)	174.34(16)	P(1)−Re−P(2)	98.62(5)	98.13(5)

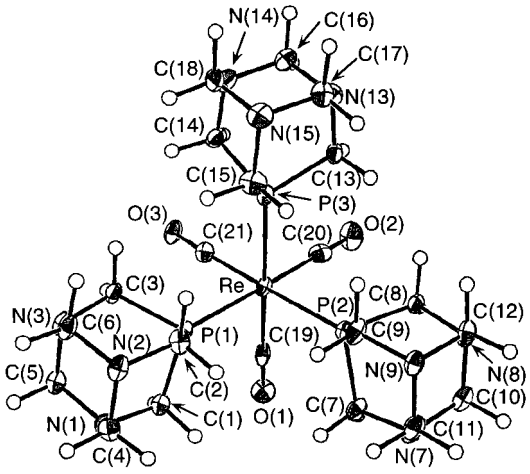

Figure 3. ORTEP drawing of the cation of $[Re(PTA)_3(CO)_3]PF_6$ (**4**) with atom numbering scheme. Ellipsoids are drawn on the 50% probability level.

Table 4. Selected Bond Lengths (Å) and Angles (deg) of Compound **4**

Re−P(1)	2.4529(19)	Re−C(19)	1.983(8)
Re−P(2)	2.4517(18)	Re−C(20)	1.963(8)
Re−P(3)	2.4383(18)	Re−C(21)	1.985(8)
P(1)−Re−P(2)	95.68(6)	P(2)−Re−C(21)	178.13(20)
P(1)−Re−P(3)	94.37(6)	P(3)−Re−C(19)	178.63(21)
P(2)−Re−P(3)	92.80(6)	P(3)−Re−C(20)	87.90(20)
P(1)−Re−C(20)	175.29(22)	P(3)−Re−C(21)	87.68(20)
P(1)−Re−C(21)	86.08(20)	C(19)−Re−C(20)	91.0(3)
P(1)−Re−C(19)	86.70(21)	C(19)−Re−C(21)	91.5(3)
P(2)−Re−C(19)	87.95(20)	C(20)−Re−C(21)	89.9(3)
P(2)−Re−C(20)	88.32(23)		

protonated nitrogen of a PTA ligand of a neighboring molecule in the unit cell (N−H···Br distances: 3.145 and 3.151 Å, respectively). Bond lengths and angles of **3b** are given in Table 3. Full details of the structure are included in the Supporting Information.

Synthesis and Characterization of $[Re(PTA)_3(CO)_3]PF_6$ (4). Complex **4** is formed only after complete substitution of the halides in **1** by weaker coordinating anion such as PF_6^- or NO_3^-. The substitution of the halides was achieved using 3 equiv of the corresponding silver salt in THF or water, respectively. Addition of 3 equiv of PTA produced the complex cation $[Re(PTA)_3(CO)_3]^+$ in good yields regardless if the reaction was performed in THF (with PF_6^- as the counterion) or in water (with NO_3^- as the counterion) as confirmed by ^{31}P NMR experiments. With NO_3^- as the counterion, complex $[Re(PTA)_3(CO)_3]^+$ is soluble in water and polar organic solvents whereas, with PF_6^- it is soluble in organic solvents only. Crystallization of the product is favored with PF_6^- as the counterion, therefore, all analytical experiments were carried out using $[Re(PTA)_3(CO)_3]PF_6$ (**4**). The ^1H and ^{13}C NMR spectra are consistent with the proposed structure. The ^{31}P NMR spectrum, in addition to the septet of PF_6^- (−144.1 ppm), presented a broad singlet at −95.3 ppm for the coordinated ligands.

Compound **4** crystallized in the triclinic space group $P\bar{1}$. An ORTEP view of the complex cation along with the atom numbering scheme is given in Figure 3. Selected bond lengths and angles are listed in Table 4. Compound **4** cocrystallized with one molecule of acetonitrile per formula unit. The P−Re−P angles have an average of 94(1)°, which is similar to the mean P−Mo−P bond angle (94(2)°) observed in the structurally comparable, neutral complex *fac*-$Mo(PTA)_3(CO)_3$.[14a]

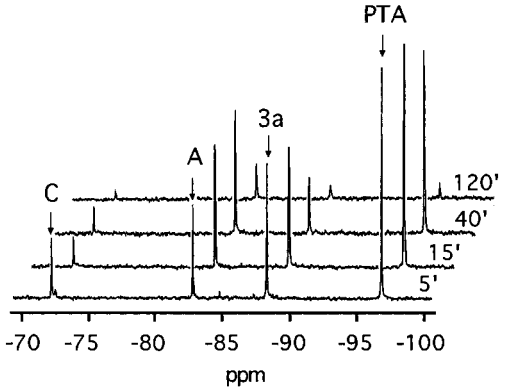

Figure 4. Time dependent ^{31}P NMR spectra of the formation of **3a** in methanol. (A) = $[ReBr(MeOH)PTA(CO)_3]$; (C) = $[Re(MeOH)(PTA)_2(CO)_3]^+$.

Scheme 2

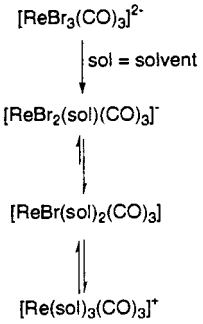

The C−Re−C bond angles have an average of 90.8(6)°. The mean Re−P bond length is 2.447(8) Å. This is only slightly longer than in the neutral complex **3a** (0.02 Å) but significantly longer than in the anionic complex **2** (0.12 Å). This observation can be explained by a weaker metal-to-ligand back-bonding in complex **4** due to the coordination of three π-accepting ligands to the metal center and the positive overall charge.

^{31}P NMR Spectroscopic Studies of Substitution Patterns in $[ReBr_3(CO)_3]^{2-}$. An important determinant in using a radiolabeled complex for nuclear medical applications is, that the complex must display thermodynamic stability and/or kinetic inertness under high dilution in aqueous media and physiological pH. The suitability of ^{188}Re-labeled PTA for radiopharmaceutical use may be understood by studying solution properties of PTA complexes of rhenium at macroscopic levels. Therefore, it is of fundamental importance to gain an insight into the substitution behavior of $[ReBr_3(CO)_3]^{2-}$, under different reaction conditions (various pH values and different solvent systems). Since ^{31}P NMR chemical shifts of metal-coordinated phosphine nuclei are sensitive to substitution around the metal center, ^{31}P NMR spectroscopy has become a reliable analytical tool to understand the coordination/substitution behavior and kinetics of phosphine−metal compounds.

Generally, $[ReBr_3(CO)_3]^{2-}$ (**1**) follows the equilibrium pattern outlined in Scheme 2. An aqueous solution of **1** showed the equilibrium completely shifted toward the formation of $[Re(OH_2)_3(CO)_3]^+$. However, IR spectroscopic experiments revealed the formation of partially solvated species $[ReBr_2(sol)(CO)_3]^-$ and $[ReBr(sol)_2(CO)_3]$ in weakly coordinating organic solvents (sol = solvent).[8]

A methanolic solution of **1**, 5 min after the addition of 2 equiv of PTA, revealed in the ^{31}P NMR spectrum, beside free PTA (−96.8 ppm) the resonances of the product $[ReBr(PTA)_2(CO)_3]$ (−88.2 ppm) and the species $[ReBr(MeOH)PTA(CO)_3]$

Scheme 3

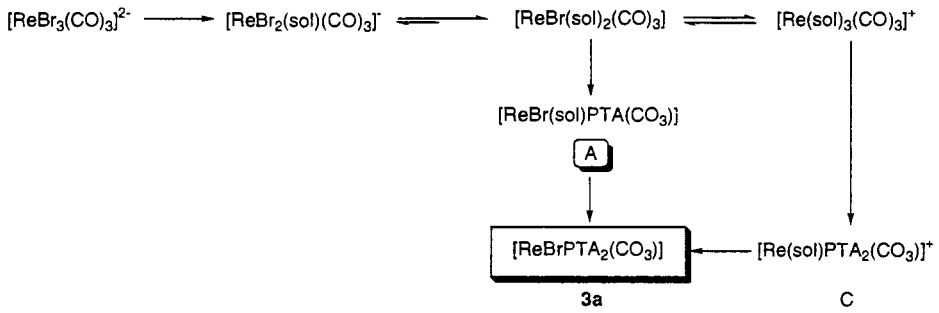

Scheme 4

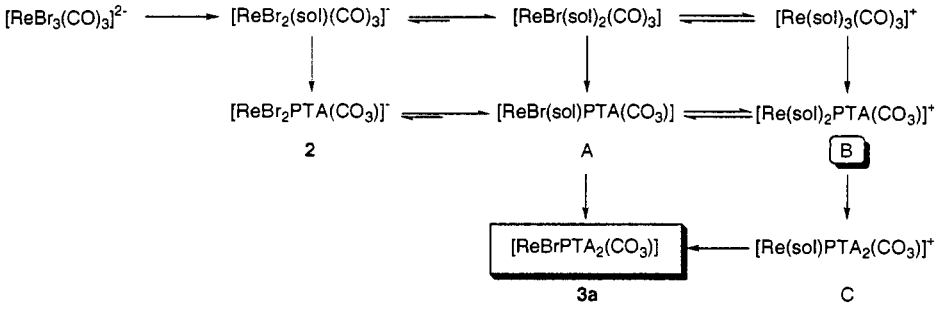

(**A**) at −82.7 ppm. The fourth signal at −72.2 ppm was tentatively assigned to the species **C**, $[Re(MeOH)(PTA)_2(CO)_3]^+$ (Figure 4). This assumption was later confirmed by the fact that addition of two equiv. of PTA to a methanolic solution of **1** (after complete exchange of the halides by weaker coordinating NO_3^- ions) showed exclusively a single signal at −72.2 ppm. Forty minutes after addition of the ligand, the intensity of the product $[ReBr(PTA)_2(CO)_3]$ decreased with the concomitant formation of a white precipitate in the NMR tube. After 2 h, the intensities of all signals were weak, confirming the almost complete formation of **3a** and its precipitation from reaction solution. The schematic sketch of the reaction mechanism as a result of the MeOH mediated solvation process is outlined in Scheme 3.

To overcome the problem associated with the precipitation of **3a**, the above reaction was performed in a solvent mixture of DMSO and methanol (4:1). After 10 min, the ^{31}P NMR spectrum consisted of six signals (Figure 5). The resonances of the final product **3a** (−89.8 ppm), species $[ReBr(DMSO)PTA(CO)_3]$ (**A**: −82.7 ppm), species $[Re(DMSO)_2PTA(CO)_3]^+$ (**B**: −85.3 ppm) and $[Re(DMSO)(PTA)_2(CO)_3]^+$ (**C**: −72.9 ppm) as well as the signal of unreacted PTA ligand (−99.9 ppm) were observed. Surprisingly, complex **2** (−87.3 ppm) was also detected. However, this peak completely disappeared after 20 min. After 4 h, the signal of the free ligand completely disappeared and the concentrations of species **A**, **B**, and **C** decreased drastically. Finally after 8 h, the ^{31}P NMR spectrum consisted of solely the signal of **3a**. The results of this experiment are outlined in Scheme 4. The formation of species **B** in DMSO, but not in methanol, can be explained by the stronger coordination capacity of DMSO toward the rhenium(I) center. Complex $[Re(DMSO)_2PTA(CO)_3]^+$ seems to be a substitutionally inert species. This might also explain the slower reaction kinetics in the DMSO/methanol mixture (8 h compared to 2 h in methanol until complete formation of **3a**).

The exclusive formation of **3a** in both cases (methanol and DMSO/methanol), even when starting with an excess of PTA ligand, can be explained by an increased electron deficiency of the rhenium(I) center after coordination of two strong π-accepting phosphine ligands. Therefore, the re-coordination of a bromine is more favored than the coordination of an additional PTA ligand. This conclusion is supported by the fact that the trisubstituted complex **4** could only be synthesized after complete exchange of the bromides. Complex $[Re(sol)(PTA)_2(CO)_3]^+$ is rapidly formed. However, the coordination of the third PTA ligand to form complex **4** is extremely slow ($T_{1/2}$ >10 h) as confirmed in the ^{31}P NMR experiment. Similar observations are reported for the reaction of **1** with the strong π-accepting ligand *tert*-butylisocyanide.[7b]

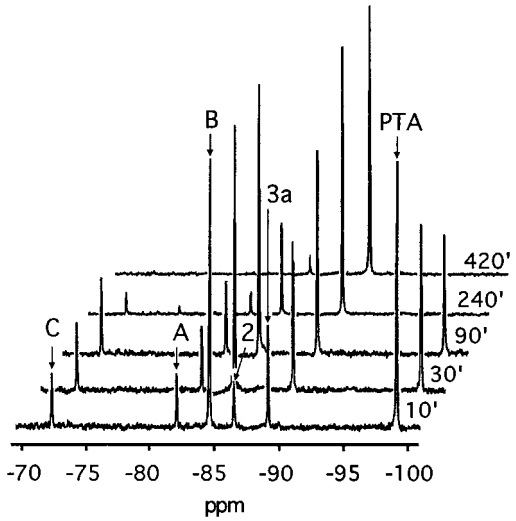

Figure 5. Time dependent ^{31}P NMR spectra of the formation of **3a** in DMSO/methanol. (A) = $[ReBr(DMSO)PTA(CO)_3]$; (B) = $[Re(DMSO)_2PTA(CO)_3]^+$; (C) = $[Re(DMSO)(PTA)_2(CO)_3]^+$.

Phase Transfer Experiments. Catalytically active transition metal complexes that are bound to ligands capable of protonation and deprotonation, will provide significant advantages in tuning the solubility characteristics of a catalyst by simply changing the pH of their solution. Examples of compounds showing pH-mediated ambivalent organic−aqueous solubility behavior include complexes of Co, Rh, Ir, and Ru with aminoalkyl-,

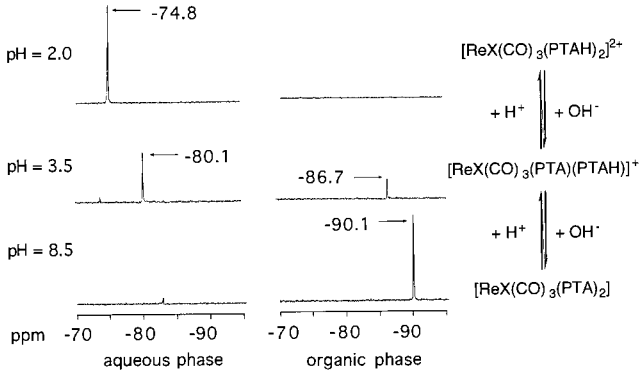

Figure 6. pH dependent ^{31}P NMR spectra of **3** under biphasic (H_2O/THF) conditions.

2-pyridylalkylphosphines, and PTA.[14b,15] Our studies on [ReBr(PTA)$_2$(CO)$_3$] (**3a**) have provided the first example of a Re(I) mixed carbonyl/PTA complex exhibiting a similar solubility behavior.

The neutral complex **3a** is insoluble in water but soluble in weakly polar organic solvents such as THF. The complex **3b** on the other hand is highly soluble in water but is only sparingly soluble in organic solvents. We layered a 2 M aqueous solution of NaBr with a saturated THF solution of **3a**. Figure 6 depicts the ^{31}P NMR spectra of the aqueous and organic phase at different pH values. The pH was adjusted using hydrobromic acid and NaOH, respectively. At pH = 2, the complex exists only in the diprotonated form **3b** in the aqueous layer, whereas at pH = 8.5 only the signal of the neutral compound **3a** could be observed in THF. At a pH of 3.5, a ^{31}P resonance was detected in both layers (−80.1 ppm in the aqueous phase and −86.7 ppm in the THF phase, respectively) presumably due to the monoprotonated species [ReBr(CO)$_3$(PTA)(PTAH)]$^+$ (**3c**). The different chemical shifts of **3c** in both layers must be solvent-related. This phase transfer reaction could be performed several times with only minor decomposition of the complex. When the system was stirred overnight at pH 8.5, small amounts of oxidized ligand O=PTA could be detected at −3.1 ppm in the ^{31}P NMR spectrum.

Conclusion

The stepwise replacement of one or more halides in **1** by the hydrophilic phosphine ligand PTA resulted in the formation of the mono-, di-, and tricoordinated compounds **2**, **3a**/**b**, and **4**. These compounds showed an ambivalent solubility behavior in organic and aqueous media. The phase transfer experiments (from aqueous to organic media and vice versa), as demonstrated for [ReBr(PTA)$_2$(CO)$_3$] (**3a**) prove the importance of protophilic ligands to achieve optimal solubility characteristics for potential application of Re(I) compounds in biphasic catalysis. Kinetically inert Re(I) complexes exhibiting good water-soluble characteristics are also important in the context of developing their ^{188}Re analogues for therapeutic application in nuclear medicine. The ability of PTA ligands to produce kinetically inert and water-soluble compounds with **1** will present further applications of this class and related derivatives of PTA in nuclear medicine.

Acknowledgment. This work was supported by the Department of Energy (DEFG0289E R60875), DuPont-Merck Pharmaceuticals, and the Departments of Chemistry and Radiology of the University of Missouri—Columbia.

Supporting Information Available: X-ray crystallographic data, in CIF format, for complexes **2**, **3a**/**b**, and **4** are available on the Internet only. Access information is given on any current masthead page.

IC980373P

(15) Andreetta, A.; Barberis, G.; Gregorio, G. *Chim. Ind.* **1978**, *60*, 887.